Title

Nonlinear optical microscopy of articular cartilage

Journal

Osteoarthritis and Cartilage, 13(4)

ISSN

1063-4584

Authors

Yeh, Alvin T

Hammer-Wilson, Marie J

Van Sickle, David C

et al.

Publication Date

2005-04-01

DOI

10.1016/j.joca.2004.12.007

OsteoArthritis and Cartilage (2005) **13,** 345–352

doi:10.1016/j.joca.2004.12.007

Osteoarthritis and Cartilage

International Cartilage Repair Society

OARSI OSTEOARTHRITIS RESEARCH SOCIETY INTERNATIONAL

Nonlinear optical microscopy of articular cartilage

Alvin T. Yeh Ph.D.†, Marie J. Hammer-Wilson M.S.‡, David C. Van Sickle D.V.M., Ph.D.§, Hilary P. Benton Ph.D.‖, Aikaterini Zoumi Ph.D.‡, Bruce J. Tromberg Ph.D.‡ and George M. Peavy D.V.M., D.A.B.V.P.‡*

† *Department of Biomedical Engineering, Texas A&M University, College Station, TX 77843, USA*

‡ *Beckman Laser Institute, University of California, Irvine, CA 94612, USA*

§ *Department of Basic Medical Sciences, Purdue University, West Lafayette, IN 47907, USA*

‖ *Department of Anatomy, Physiology & Cell Biology, School of Veterinary Medicine, University of California, Davis, CA 95616, USA*

Summary

Objective: To assess the ability of nonlinear optical microscopy (NLOM) to image *ex vivo* healthy and degenerative bovine articular cartilage.

Method: Fresh bovine femoral–tibial joints were obtained from an abattoir. Articular cartilage specimens were harvested from the tibial plateau. Normal and degenerative specimens were imaged by NLOM and subsequently fixed and processed for histological examination.

Results: NLOM provided high resolution images of articular cartilage at varying depths with high sensitivity to tissue morphology and high specificity to tissue components without fixing, sectioning or staining. Spectroscopic segmentation of nonlinear optical signals isolated the collagen matrix from the chondron (chondrocyte and non-collagen pericellular matrix). Images from the superficial zone were consistent with the presence of a matrix composed of both elastin-like and collagen fibers distributed in a depth-dependent morphological arrangement, whereas only collagen was demonstrated in the middle and deep zones. Alterations of collagen matrix associated with advanced degenerative joint disease (fibrocartilage) were observed with NLOM. Individual chondrocytes were imaged and demonstrated intracellular fluorescence consistent with the presence of products of intracellular biochemical processes.

Conclusion: Thin images of living articular cartilage using NLOM may be obtained with (sub-)cellular resolution at varying depths without fixing, sectioning or staining. Extracellular matrical collagen and chondron may be imaged separately in native tissue using spectrally distinct, endogenous, nonlinear optical signals. NLOM was sensitive to macromolecular composition and pathologic changes in articular cartilage matrix. Advances in instrumentation may lead to the application of NLOM to study articular cartilage *in vivo*.

Key words: Articular, Cartilage, Degenerative joint disease, Collagen, Elastin, Multiphoton microscopy, Second-harmonic generation, Arthritis, Orthopedic surgery, Chondrocyte.

Introduction

The functional properties of cartilage are dependent on a complex extracellular matrix which is produced and maintained by the cellular component, chondrocytes[1,2]. In the synovial joint, articular cartilage absorbs impact and distributes loads during movement, providing smooth articulation and protection for underlying bone. Endogenous articular chondrocytes are maintained in a three-dimensional (3-D) structure encapsulated in a highly organized matrix.

Major matrical components are negatively charged proteoglycans (glycosaminoglycans attached to a protein backbone) aggregated to a strand of hyaluronic acid (aggrecan) and secondarily attached to type II collagen. In addition, there are a number of smaller matrical molecules with significant functions in maintaining tissue organization. The interplay of polyanionic, aggregating proteoglycans, cations and water lead to interstitial swelling and the ability to resist compressive deformation[3–5] while the collagenous framework provides resistance against tensile deformation[6].

In diseased states such as osteoarthritis, cartilage matrix is damaged with progressive loss of architectural integrity, cell death, alterations in composition and compromise of biomechanical function, resulting in joint stiffness and pain. A histological–histochemical grading system and various modifications of it are widely used to describe these progressive changes[7]. There have been enormous advances in understanding molecular mechanisms responsible for degradation and release of cartilage matrix components, however, visualizing these complex processes within intact tissue remains challenging.

Conventional light, electron and immunohistochemical microscopy have identified a high degree of organization within the structure of the matrix and distinct matrical differences in cellular arrangement and extracellular architecture within different zones and spatial locations[8]. The destructive nature of these techniques often precludes serial, time-dependent studies on biological processes responsible for tissue maintenance, repair and degeneration

*Address correspondence and reprint requests to: George M. Peavy, D.V.M., D.A.B.V.P., Beckman Laser Institute, University of California, 1002 Health Sciences Road East, Irvine, CA 92612, USA. Tel: 1-949-824-4713; Fax: 1-949-824-8413; E-mail: gpeavy@uci.edu

Received 17 July 2004; revision accepted 24 December 2004.

except in specific situations. For example, a novel application of differential interference contrast microscopy has been used to monitor chondrocyte dynamics in living growth plate cartilage explants without fixation and staining. However, because this technique involved light transmission from illumination source through tissue to an imaging objective, sections of specimens 100–200 μm in thickness were required in order for visualization from the imaging plane without disturbance of the optical beam[9].

High resolution imaging utilizing intrinsic optical signals from cartilage matrix components and chondrocytes in intact living tissue without the need for sectioning, preparation or staining would allow an improved study of chondrocyte and matrix physiology with fewer artifacts. Such technology could aid in early detection of disease during arthroscopy and in evaluation of chondrocytic function and matrix integrity in tissue engineered cartilage constructs[10] or cartilage generated by transplanted chondrocytes. Presently, clinical non-invasive techniques such as magnetic resonance imaging and ultrasound lack resolution needed to distinguish complex structures of articular cartilage, although sensitivity and applicability of these techniques continue to improve and expand[11]. Arthroscopy remains a very useful, minimally invasive technique but only provides information about cartilage structure at articular surfaces and requires anesthesia and surgery[12]. Optical coherence tomography provides full thickness, high resolution (~10 μm), cross-sectional images of cartilage, but lacks the ability to distinguish among biological constituents[13–16]. While laser scanning confocal microscopy has phototoxicity problems for imaging hard tissues, nonlinear optical microscopy (NLOM) continues to prove useful for imaging live tissues with minimal toxicity[17,18].

In an earlier study, we used NLOM to image nasal septal cartilage which allowed visualization of chondrocytes in their 3-D matrix environment[19]. NLOM has been combined with fluorescent calcium imaging probes to visualize ion movement within endothelial cells of blood vessel walls[20]. In this study, we used NLOM to image chondrocytes and matrical components of live, intact articular cartilage in both normal and pathological states.

NLOM is a non-destructive, laser scanning microscopy technique that renders images of living tissue with (sub-) cellular resolution and component specificity without use of exogenous stains or dyes. Using backreflected experimental geometry, NLOM is not limited by sample thickness. NLOM is very sensitive in defining extracellular matrix morphology[21–23]. Nonlinear optical properties of fresh, *ex vivo* bovine cartilage matrix from normal and joints demonstrating evidence of degenerative joint disease are investigated as well as depth-dependent changes in tissue morphology and composition.

Materials and methods

SPECIMEN COLLECTION AND PREPARATION

Degenerative joint disease in the bovine demonstrates many of the same histological and histochemical features of human osteoarthritis as described by Mankin[7], and provides an easily accessible source of normal and pathological articular cartilage in various stages of degeneration. Bovine articular cartilage for this study was collected from adult (5–7 years old) Holstein dairy cows slaughtered within the prior 36 h and maintained under refrigeration. Femoral–tibial joints were isolated and dissected to expose the joint surface from which a total of 12 specimens were harvested from tibial plateau, femoral condyle and patella. Samples for study were obtained from areas determined by visual examination to be either normal ($n = 4$) or in various stages of degenerative joint disease ($n = 8$) as evidenced by surface irregularities and partial to full thickness erosions of articular cartilage with fibrocartilage.

A 4 mm diameter circular punch and mallet were used to obtain core specimen samples composed of full thickness cartilage attached to subchondral bone from each site selected for study. After removal, each specimen was wrapped in a gauze sponge soaked in 0.9% saline solution, placed in a sealed container and stored at 4 °C. NLOM imaging was performed within 24 h of harvesting.

At the time of NLOM imaging, articular cartilage of each specimen was incised twice, each cut was made across the surface and parallel to each other, 1 mm apart, using a #10 scalpel blade from the surface to the subchondral bone. The two outer semicircular cartilage specimens created in this manner were elevated from the subchondral bone (Fig. 1), held in 0.9% saline soaked gauze and immediately examined by NLOM imaging.

NONLINEAR OPTICAL MICROSCOPY (NLOM)

The system has been described previously[24]. Briefly, 150 fs laser pulses centered at 800 nm with a repetition rate of 76 MHz from a Ti:Al_2O_3 oscillator pumped by a frequency doubled Nd:YVO_4 solid state laser were coupled into an inverted microscope via dual axis galvanometer mirrors. Samples were placed on a coverslip and mounted on the microscope stage. NLOM images were obtained from both articular and cut surfaces of unfixed and unstained cartilage specimens. Nonlinear optical signals were collected by the focusing objective and directed to either a spectrometer or photomultiplier tube (PMT). In the spectrometer, light was

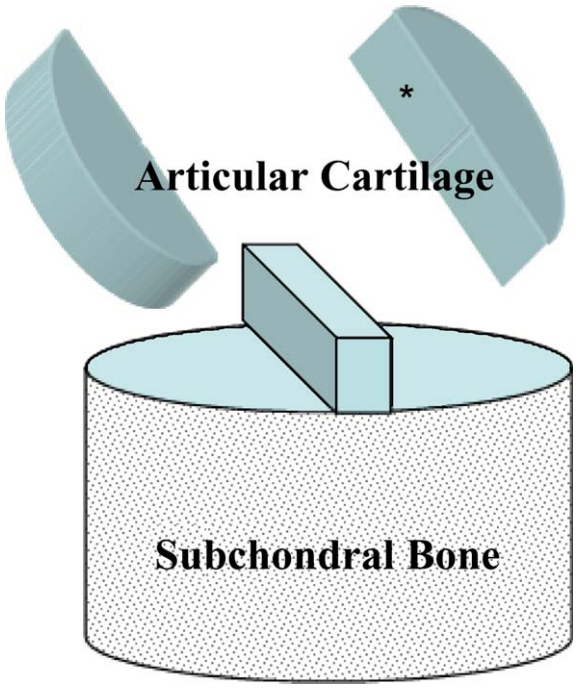

Fig. 1. Schematic of articular cartilage sample preparation for NLOM imaging. Images were obtained from articular and cut surface (asterisk).

spectrally dispersed with a grating blazed for 500 nm with 300 grooves/mm and detected using an electrically cooled charge-coupled device. Bandpass filters at 400 and 520 nm were placed in front of the PMT for image rendering using second-harmonic generation (SHG) or two-photon excited fluorescence (TPF), respectively. A Schott color glass filter (390–570 nm, FWHM) was used for intensity image rendering transmitting both SHG and TPF to the PMT. The scan rate of a single NLOM frame (256 × 256) was approximately 0.25 Hz. The images presented were an accumulation of 10 scans.

HISTOCHEMICAL STAINING

Following NLOM imaging, each specimen was placed in 10% buffered formalin, dehydrated through a graded alcohol series, embedded in paraffin, cut perpendicular to the articular and parallel to the incised surface at 5 μm intervals and mounted on 1 × 3 inch glass slides. Alternating sections were stained with Hematoxylin and Eosin-y (H&E) or safranin-O counter stained with Fast Green FCF (SOFG), or, in some selected cases, Verhoeff's stain. Prepared specimens were examined by light microscopy, and digital images were obtained of areas representative of those imaged by NLOM. Histological–histochemical characteristics of structure and safranin-O staining of Mankin's grading system[7] were used to identify characteristics of articular cartilage degeneration in specimens of this study. Light microscopy and NLOM images of similar areas of the same cartilage specimen were matched and compared.

Results

A representative full thickness histologic section through a segment of articular cartilage is shown in Fig. 2. The full thickness section stained with H&E [Fig. 2(A)] reveals morphologically distinct regions from surface to junction with subchondral bone. Higher magnification of the superficial zone [Fig. 2(B)] confirms a relatively amorphous extracellular matrix populated with chondrocytes. High magnification of the deep zone tide mark and zone of calcified cartilage [Fig. 2(C)] obtained from a different specimen stained with Alcian blue demonstrates collagen matrix anchored in calcified cartilage devoid of proteoglycans.

TPF AND SHG IMAGING OF ARTICULAR CARTILAGE

A representative spectrum of endogenous, nonlinear optical signals used for imaging is shown in Fig. 3. The spectrum was accumulated over the entire image of Fig. 3(A). It reveals a sharp peak at 400 nm (exactly half the excitation wavelength) and a broad spectral feature characteristic of TPF. The sharp peak at 400 nm has a quadratic dependence on incident laser intensity and shifts with changes in laser frequency to remain at exactly half the excitation wavelength.

Spectral dependence of the imaging signals may be used to separate biological constituents within the field of view. Shown in Fig. 3(A) is an image of two chondrocytes within articular cartilage matrix. By placing a bandpass filter at the second harmonic of the excitation wavelength (400 nm) in front of the detector, frequency doubled signal (SHG) from collagen is isolated for imaging [Fig. 3(B)]. The SHG filtered image clearly demonstrates lacuna occupied by chondrocytes and their relationship to hyaline collagen matrix. Components of chondrocyte and non-collagenous pericellular matrix may be imaged using a bandpass filter (520 nm) within the TPF spectral profile [Fig. 3(C)]. Histologically, these components correlate with the chondron. Intracellular fluorescence originates from pyridine nucleotides and/or flavoproteins of the metabolic cycle, as identified in previous work[25]. The origin of fluorescence from pericellular matrix has not been identified but may be related to proteoglycan content.

COMPARISON OF NORMAL AND DEGENERATIVE CARTILAGE BY NLOM AND HISTOLOGY

NLOM images of normal (A, B) and degenerative (C) articular cartilage using SHG and TPF and corresponding SOFG stained histology are shown in Fig. 4. In the top row, NLOM images, using a bandpass filter at 400 nm, isolate SHG from hyaline collagen, which surrounds the space occupied by a chondrocyte (lacuna). Corresponding chondrocyte images using TPF (bandpass filter at 520 nm) are shown below. Pericellular fluorescence is markedly reduced in degenerative (C) compared with normal (A, B) articular cartilage. These images have been displayed on the same intensity scale for comparison. As a reference, SOFG stained histology (shown at 25× magnification) of corresponding specimens are shown in the bottom row. Normal

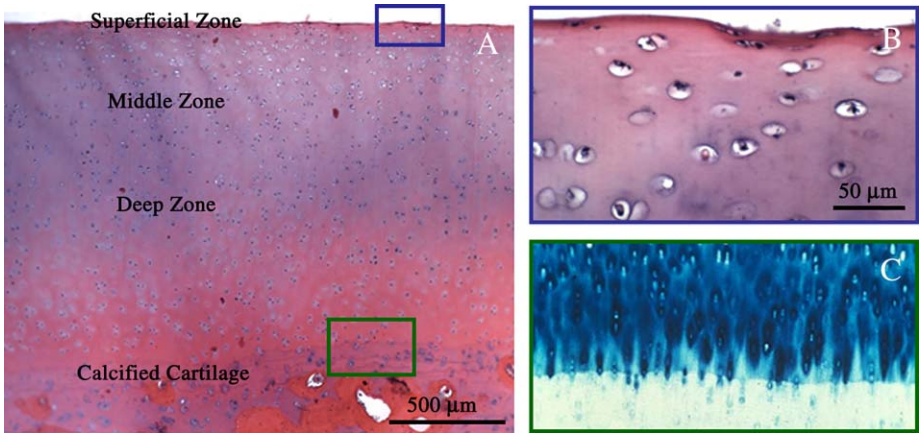

Fig. 2. Histology of articular cartilage showing (A) full thickness, (B) superficial region and (C) boundary between non-calcified and calcified cartilage.

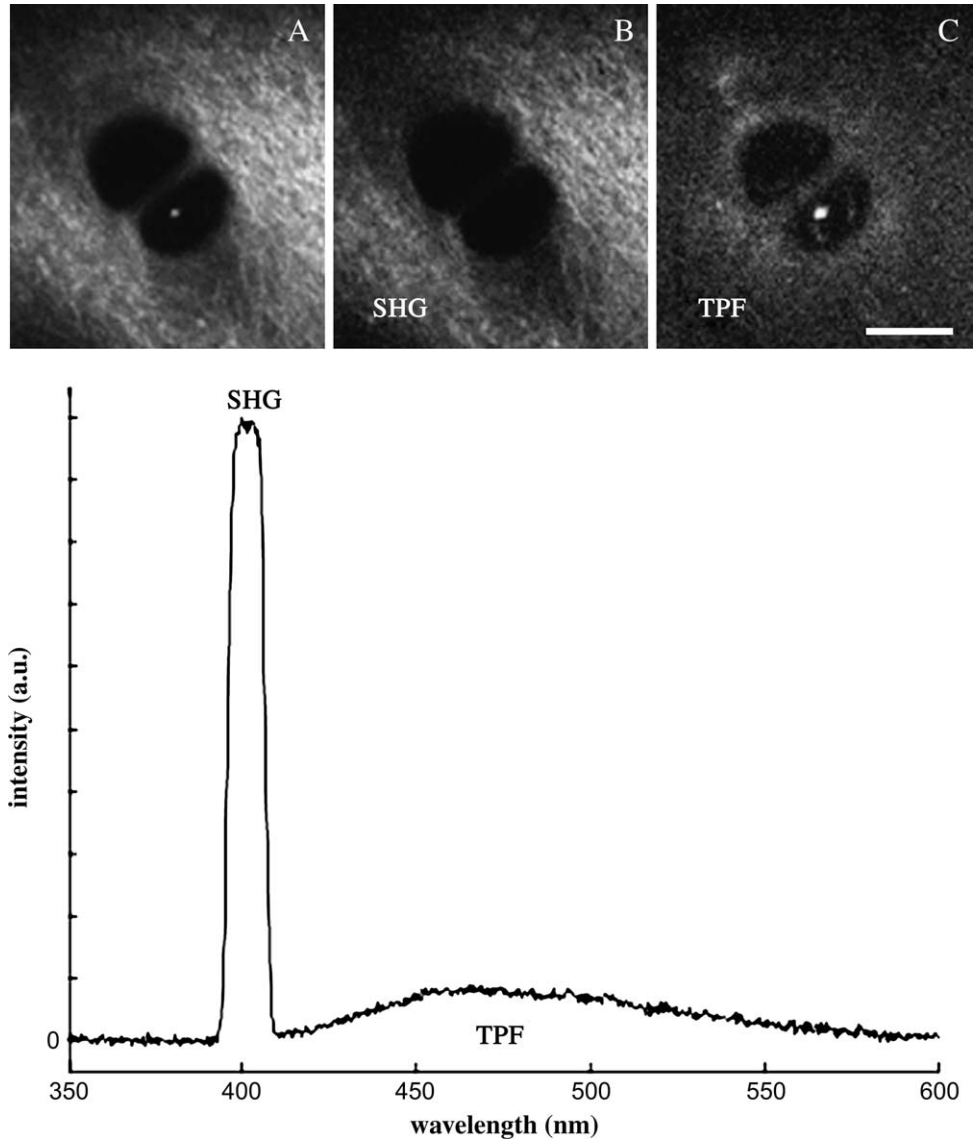

Fig. 3. Spectra of endogenous nonlinear optical signals in articular cartilage used for imaging. (A) Intensity image of chondrocytes within cartilage matrix. (B) Spectral filtering of SHG signal at 400 nm specifically imaging collagen. (C) Spectral filtering of TPF signal at 520 nm specifically imaging the chondron. Scale bar is 8 μm.

articular cartilage in Fig. 4(A and B) stains orange indicating the presence of proteoglycans. Cartilage in Fig. 4(C) shows a degenerate superficial layer and normal hyaline cartilage architecture in the middle and deep zones with a marked reduction in proteoglycan content as indicated by the absence of safranin-O staining. Variations between SOFG stained histology sections of normal and degenerative cartilage correspond to differences in extracellular TPF intensity suggesting that pericellular fluorescence in NLOM images may be related to proteoglycan content.

DEMONSTRATION OF TWO FIBER COMPONENTS IN THE SUPERFICIAL ZONE OF ARTICULAR CARTILAGE

NLOM can be sensitive to particular components of extracellular matrix. Figure 5 shows a highly magnified Verhoeff's stained section of articular cartilage as well as NLOM images from superficial and middle zones. Gray coloration in the histology section demonstrates elastin-like layers at the articular surface that are not observed in deeper regions of the tissue. Spectroscopic segmentation of NLOM images demonstrates two different fibrous structures within the superficial zone.

Each row of Fig. 5 consists of images obtained at the same focal plane and includes total intensity (SHG + TPF), TPF and SHG images arranged in columns. Intensity images (column A) show fibrous structures at shallow depths from the surface that become less prevalent and eventually disappear near the middle and into the deep zone. TPF images (column B) show that these fibrous structures are distinctly different from collagen that is imaged using SHG (column C). SHG imaging (column C) demonstrates hyaline collagen matrix. SHG images show a fibrous (collagen) structure near the surface becoming more

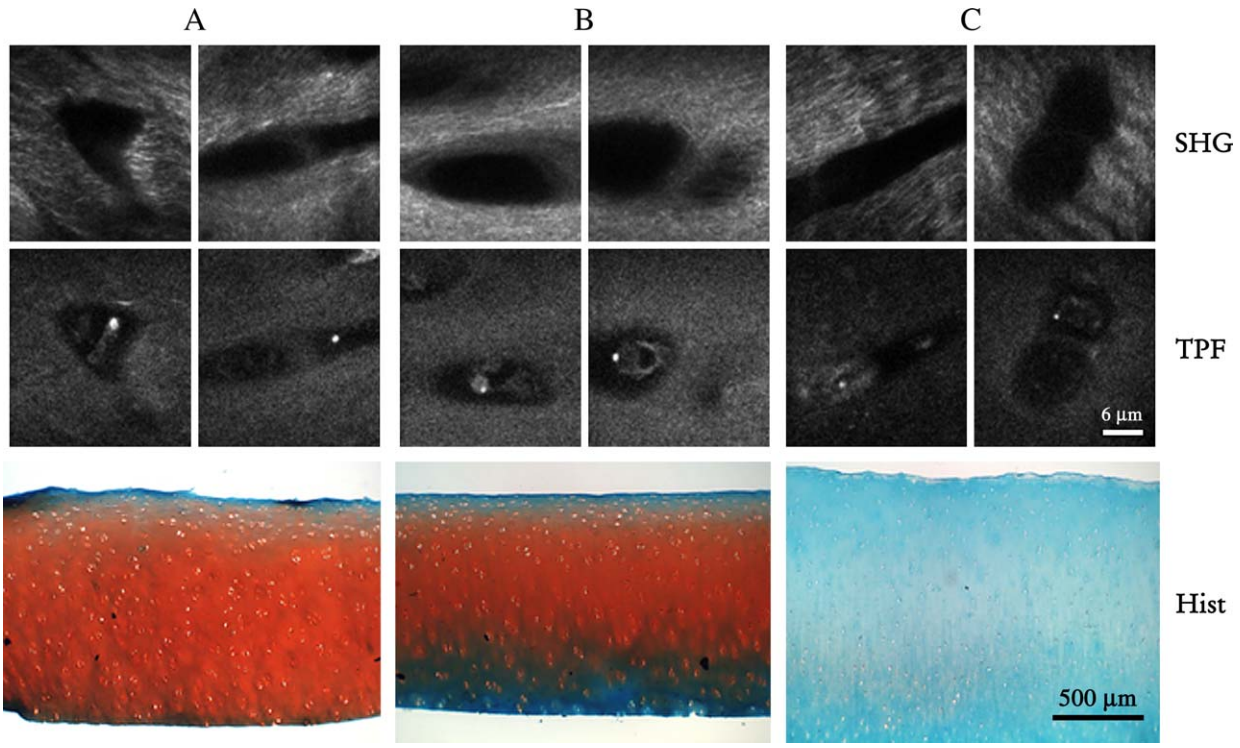

Fig. 4. NLOM images (SHG and TPF) and SOFG stained histology of normal (A, B) and degenerative joint diseased (C) articular cartilage. Extracellular TPF corresponds with proteoglycan content (orange staining).

amorphous at depth. Our previous work has shown that 800 nm excitation as used in this study will not result in collagen type I or II (auto)fluorescence[24]. In addition, fluorescent fibers observed with 800 nm excitation do not co-register with collagen visualized using SHG from the same imaging plane.

Stacks of serial NLOM images can be used to construct 3-D images of tissue. Figure 6 shows 3-D reconstructions obtained from images sequentially acquired 0.2 μm apart in depth from within the superficial zone of normal bovine articular cartilage. This 3-D reconstruction further demonstrates that fluorescing fibrous structures of the superficial zone observed by TPF are filaments distinct from collagen fibers imaged by SHG.

NLOM DEMONSTRATION OF FIBRILLAR-LIKE MATRIX STRUCTURE IN DEGENERATIVE CARTILAGE

Histology of normal articular cartilage is shown in Fig. 7(A) with NLOM intensity and vertically and horizontally polarized SHG images. No analyzer was used in the detection path. Polarization dependence of collagen SHG intensity is not observed. Early degenerative joint disease shows separation or fibrillation of hyaline cartilage [Fig. 7(B)]. This is supported by NLOM images where fibrillar-like matrix structure [Fig. 7(B and C)] rather than amorphous morphology of normal cartilage [Fig. 7(A)] is observed. Advanced degenerative joint disease is characterized by fibrocartilage tissue replacing hyaline cartilage [Fig. 7(C)]. The NLOM images of specimens B and C (Fig. 7) show fibrillar-like matrix structure (column 1) and highlight vertically and horizontally oriented fibers using vertical (column 2) and horizontal (column 3) incident laser polarizations.

Discussion

The ability of NLOM to image thin planes within full thickness articular cartilage without sectioning or using exogenous stains or dyes is demonstrated. Nonlinear optical spectroscopy of articular cartilage contains endogenous signals from chondrocytes, collagen and other pericellular and superficial matrical components. A sharp peak was observed in addition to broad, featureless fluorescence that has a quadratic dependence on incident laser intensity and shifts with changes in laser frequency to remain at exactly half the excitation wavelength. This spectroscopic feature has been observed in other collagenous tissues and is characteristic of SHG in collagen[18,21–24].

For particular excitation wavelengths, endogenous nonlinear optical signals are spectrally separable, allowing image segmentation by tissue component. Autofluorescence from collagen and elastin originate from covalent cross-links (pyridinoline and iso/desmosine, respectively) with spectrally broad, overlapping, featureless profiles[26]. Our previous work demonstrates that excitation at 800 nm results in collagen SHG but not fluorescence[24]. Excitation at 800 nm has been used for specific NLOM imaging of elastin by TPF and collagen by SHG in fixed coronary arteries[27]. Fluorescing fibrous structure revealed by TPF imaging is suggestive of an elastin-like substance and is supported by observations made from Verhoeff's stained histology sections. Additional studies are warranted to confirm the composition of unique fluorescing fibrous structure within the superficial zone of articular cartilage.

Depth-varying morphology of extracellular matrix is likely related to structural and functional requirements needed to resist forces generated in articular tissue during weight bearing motion. Previous work has shown that octahedral stress and tensile strain predominate near the surface with

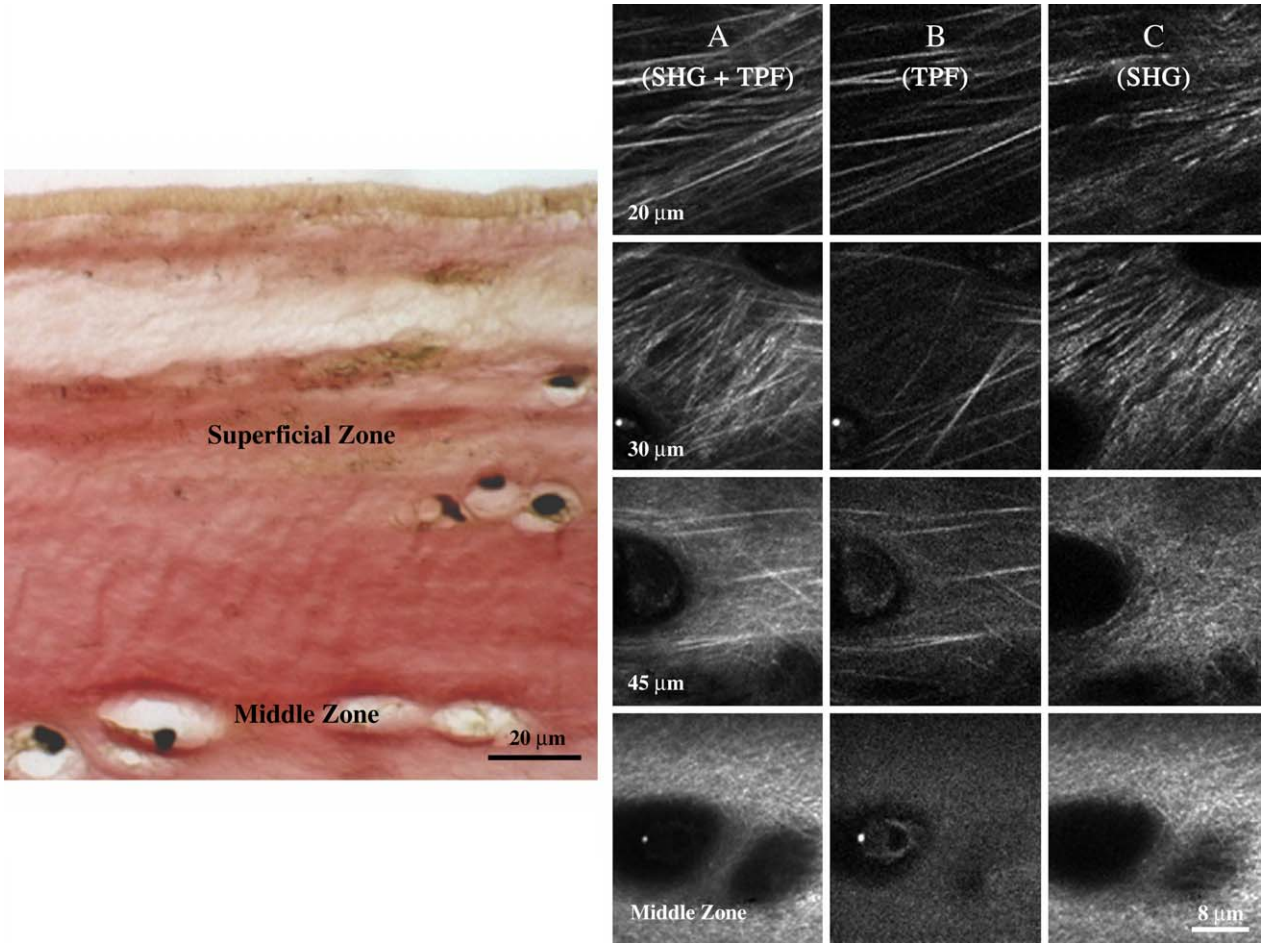

Fig. 5. Verhoeff's stained histology suggesting the presence of elastin (gray fibers) within the superficial layer. Depth-dependent intensity (SHG + TPF), TPF and SHG images showing ability to segment elastin-like fibers (TPF) and collagen (SHG) near the articular surface and matrix compositional and morphological changes with depth.

hydrostatic compressive forces dominating below the surface layers[28,29]. This might tautologically explain both regional differences in the presence of elastin-like fibrous structures and collagen fiber orientation.

SHG in fibrillar collagens, particularly type I, has been shown to have polarization dependence with incident laser electric field. Its second-order polarizability has been shown to be dominated by a component along the fiber axis[30,31].

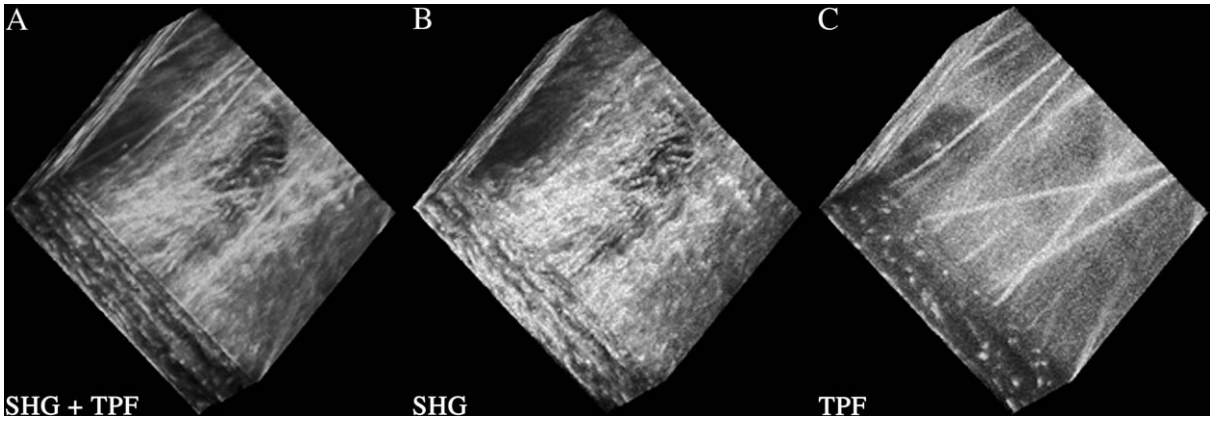

Fig. 6. NLOM images composed of (A) combined SHG and TPF, (B) SHG and (C) TPF signals obtained at 0.2 μm intervals through a 32 μm × 30 μm × 14 μm volume of the superficial zone of normal bovine articular cartilage are stacked to provide a 3-D image of the tissue. The images constructed here demonstrate that fluorescing fibrous structures of the superficial zone observed by TPF are distinct from collagen imaged by SHG.

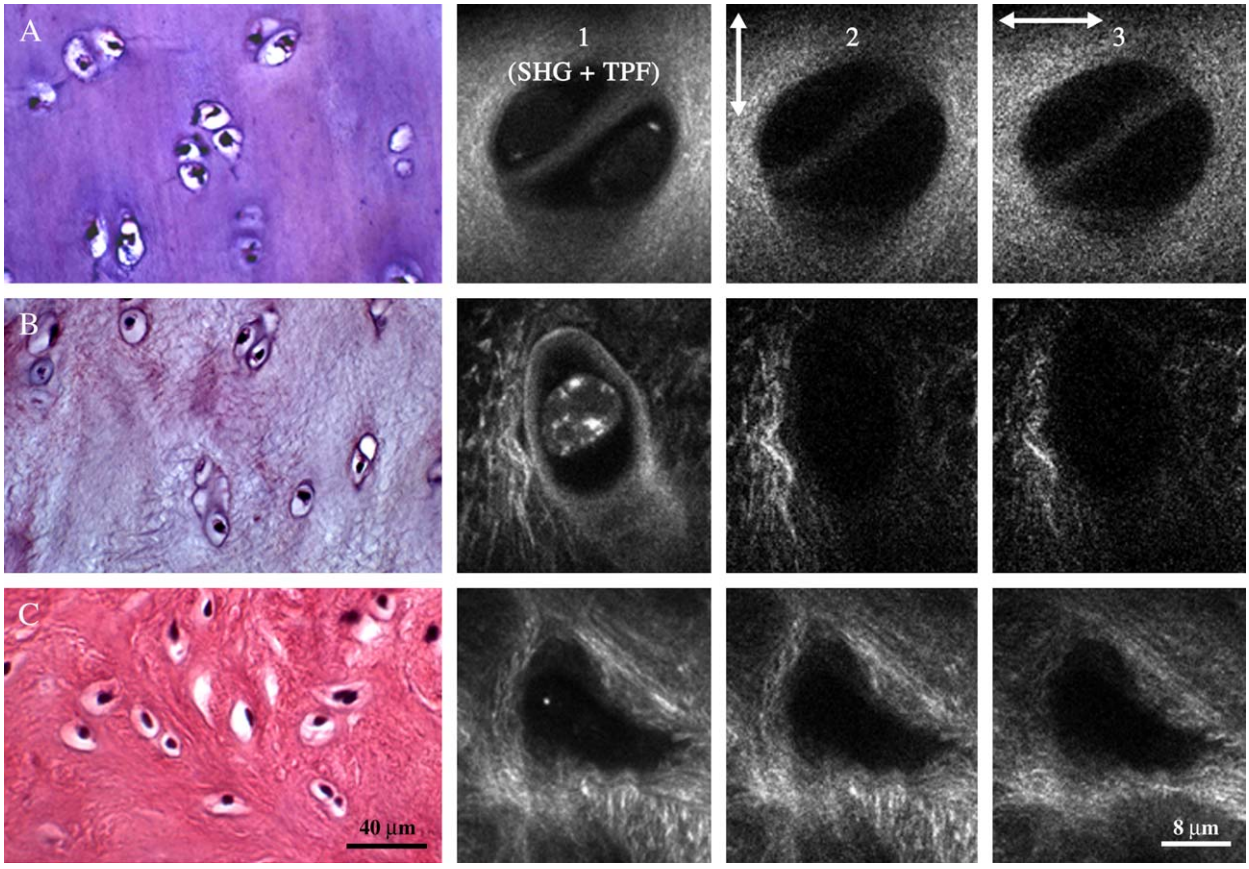

Fig. 7. Histology and NLOM images of (A) normal, (B) early fibrillar matrical degeneration and (C) fibrocartilage of advanced degenerative joint disease. Intensity (column 1) and SHG NLOM images using vertically (column 2) and horizontally (column 3) polarized incident laser light are shown.

Consequently, polarization of the incident electric field may be used to enhance NLOM imaging of collagen orientation within tissues[22]. However, hyaline cartilage is composed of type II collagen and may have distinct SHG behavior because of its macroscopic arrangement. The polarization dependence of SHG in normal articular cartilage was investigated and a dominant uniaxial component was not observed. We speculate this is due to the length scale of collagen molecular order in hyaline cartilage relative to the wavelength of the incident laser. However, degenerative joint disease may result in fibrillation of hyaline cartilage (early) or metaplasia to fibrocartilage (advanced) leading to observable polarization dependence in collagen SHG. SHG in fibrocartilage was particularly sensitive to incident laser polarization as shown in Fig. 7(C).

The ability to visualize particular tissue constituents with (sub-)cellular resolution and without need for sectioning shows great potential for non-destructive monitoring of fundamental cartilage biology in terms of tissue homeostasis and initiation and progression of degenerative joint disease. Our results suggest that with advances in instrumentation, NLOM has potential to assist in future studies of basic biological processes in living, full thickness articular cartilage with the ability to detect changes in chondrocyte–matrix interactions leading to joint disease.

Acknowledgments

We are pleased to acknowledge Dr Brian J.F. Wong for helpful comments and review of the manuscript and Angela Liogys and Sharon Evander for assisting with histology. This work was supported by the National Center for Research Resources of the National Institutes of Health (Laser Microbeam and Medical Program, RR-01192), the U.S. Air Force Office of Scientific Research, Medical Free-Electron Laser (F49620-00-1-0371) and the Arnold and Mabel Beckman Foundation. The U.S. Government is authorized to reproduce and distribute reprints for Governmental purposes notwithstanding any copyright notation. The views and conclusions contained herein are those of the authors and should not be interpreted as necessarily representing the official policies or endorsements, either expressed or implied, of the Air Force Research Laboratory or the U.S. Government.

References

1. Muir H. The chondrocyte, architect of cartilage. Biomechanics, structure, function and molecular biology of cartilage matrix macromolecules. Bioessays 1995; 17(12):1039–48.
2. Lai WM, Hou JS, Mow VC. A triphasic theory for the swelling and deformation behaviors of articular cartilage. J Biomech Eng 1991;113:245–58.
3. Hardingham TE, Beardmore-Gray M, Dunham DG, Ratcliffe A. Cartilage proteoglycans. Ciba Found Symp 1986;124:30–46.

4. Maroudas A, Bannon C. Measurement of swelling pressure in cartilage and comparison with the osmotic pressure of constituent proteoglycans. Biorheology 1981;18(3–6):619–32.
5. Urban JP, Maroudas A, Bayliss MT, Dillon J. Swelling pressures of proteoglycans at the concentrations found in cartilaginous tissues. Biorheology 1979; 16(6):447–64.
6. Kuhn K. Structural and functional domains of collagen: a comparison of the protein with its gene. Collagen Relat Res 1984;4(4):309–22.
7. Mankin HJ, Dorfman H, Lippiello L, Zarins A. Biochemical and metabolic abnormalities in articular cartilage from osteo-arthritic human hips. II. Correlation of morphology with biochemical and metabolic data. J Bone Joint Surg Am 1971;53(3):523–37.
8. Kincaid SA, Van Sickle DC. Regional histochemical and thickness variations of adult canine articular cartilage. Am J Vet Res 1981;42:428–32.
9. Farnum CE, Turgai J, Wilsman NJ. Visualization of living terminal hypertrophic chondrocytes of growth plate cartilage *in situ* by differential interference contrast microscopy and time-lapse cinematography. J Orthop Res 1990;8:750–63.
10. Garfein ES, Orgill DP, Pribaz JJ. Clinical applications of tissue engineered constructs. Clin Plast Surg 2003; 30(4):485–98.
11. Gold GE, McCauley TR, Gray ML, Disler DG. What's new in cartilage? Radiographics 2003;23(5):1227–42.
12. Tuijthof GJ, van Dijk CN, Herder JL, Pistecky PV. Clinically-driven approach to improve arthroscopic techniques. Knee Surg Sports Traumatol Arthrosc 2005;13(1):48–54.
13. Herrmann JM, Pitris C, Bouma BE, Boppart SA, Jesser CA, Stamper DL, *et al*. High resolution imaging of normal and osteoarthritic cartilage with optical coherence tomography. J Rheumatol 1999;26(3): 627–35.
14. Roberts MJ, Adams SB Jr, Patel NA, Stamper DL, Westmore MS, Martin SD, *et al*. A new approach for assessing early osteoarthritis in the rat. Anal Bioanal Chem 2003;377(6):1003–6.
15. Rogowska J, Bryant CM, Brezinski ME. Cartilage thickness measurements from optical coherence tomography. J Opt Soc Am A 2003;20(2):357–67.
16. Pan Y, Li Z, Xie T, Chu CR. Hand-held arthroscopic optical coherence tomography for *in vivo* high-resolution imaging of articular cartilage. J Biomed Opt 2003; 8(4):648–54.
17. Watson TF, Azzopardi A, Etman M, Cheng PC, Sidhu SK. Confocal and multi-photon microscopy of dental hard tissues and biomaterials. Am J Dent 2000; 13(Spec. No.):19D–24D.
18. Campagnola PJ, Loew LM. Second-harmonic imaging microscopy for visualizing biomolecular arrays in cells, tissues and organelles. Nat Biotechnol 2003;21: 1356–60.
19. Wong BJF, Wallace V, Coleno M, Benton HP, Tromberg BJ. Two-photon excitation laser scanning microscopy of human, porcine and rabbit nasal septal cartilage. Tissue Eng 2001;7(5):599–606.
20. Ohata H, Yamada H, Niioka T, Yamamoto M, Momose K. Optical bioimaging: from living tissue to a single molecule: calcium imaging in blood vessel *in situ* employing two-photon excitation fluorescence microscopy. J Pharmacol Sci 2003;93(3):242–7.
21. Cox G, Kable E, Jones A, Fraser I, Manconi F, Gorrell MD. 3-Dimensional imaging of collagen using second harmonic generation. J Struct Biol 2003;141:53–62.
22. Yeh AT, Nassif N, Zoumi A, Tromberg BJ. Selective corneal imaging using combined second harmonic generation and two-photon excited fluorescence. Opt Lett 2002;27(23):2082–4.
23. Zipfel WR, Williams RM, Christie R, Nikitin AY, Hyman BT, Webb WW. Live tissue intrinsic emission microscopy using multiphoton-excited native fluorescence and second harmonic generation. Proc Natl Acad Sci U S A 2003;100(12):7075–80.
24. Zoumi A, Yeh A, Tromberg BJ. Imaging cells and extracellular matrix *in vivo* by using second-harmonic generation and two-photon excited fluorescence. Proc Natl Acad Sci U S A 2002;99(17):11014–9.
25. Huang S, Heikal AA, Webb WW. Two-photon fluorescence spectroscopy and microscopy of NAD(P)H and flavoprotein. Biophys J 2002;82:2811–25.
26. Wagnieres GA, Star WM, Wilson BC. *In vivo* fluorescence spectroscopy and imaging for oncological applications. Photochem Photobiol 1998;68(5): 603–32.
27. Zoumi A, Lu X, Kassab GS, Tromberg BJ. Imaging coronary artery microstructure using second-harmonic and two-photon fluorescence microscopy. Biophys J 2004;87:2778–86.
28. Vanwanseele B, Lucchinetti E, Stussi E. The effects of immobilization on the characteristics of articular cartilage: current concepts and future directions. Osteoarthritis Cartilage 2002;10:408–19.
29. Carter DR, Wong M. Modelling cartilage mechanobiology. Philos Trans R Soc Lond B 2003;358:1461–71.
30. Stoller P, Kim B-M, Rubenchik AM, Reiser KM, Silva LBD. Polarization-dependent optical second-harmonic imaging of a rat-tail tendon. J Biomed Opt 2002;7(2): 1–10.
31. Stoller P, Reiser KM, Celliers PM, Rubenchik AM. Polarization-modulated second harmonic generation in collagen. Biophys J 2002;82:3330–42.